Nanoscale

PAPER

View Article Online
View Journal

Cite this: DOI: 10.1039/c7nr08294k

Sensing local pH and ion concentration at graphene electrode surfaces using *in situ* Raman spectroscopy†

Haotian Shi,[a] Nirakar Poudel,[b] Bingya Hou,[b] Lang Shen,[c] Jihan Chen,[b] Alexander V. Benderskii[a] and Stephen B. Cronin *[a,b]

Received 7th November 2017,
Accepted 10th December 2017

DOI: 10.1039/c7nr08294k

rsc.li/nanoscale

We report a novel approach to probe the local ion concentration at graphene/water interfaces using *in situ* Raman spectroscopy. Here, the upshifts observed in the G band Raman mode under applied electrochemical potentials are used to determine the charge density in the graphene sheet. For voltages up to ±0.8 V *vs.* NHE, we observe substantial upshifts in the G band Raman mode by as much as 19 cm^{-1}, which corresponds to electron and hole carrier densities of 1.4 × 10^{13} cm^{-2} and Fermi energy shifts of ±430 meV. The charge density in the graphene electrode is also measured independently using the capacitance–voltage characteristics (*i.e.*, $Q = CV$), and is found to be consistent with those measured by Raman spectroscopy. From charge neutrality requirements, the ion concentration in solution per unit area must be equal and opposite to the charge density in the graphene electrode. Based on these charge densities, we estimate the local ion concentration as a function of electrochemical potential in both pure DI water and 1 M KCl solutions, which span a pH range from 3.8 to 10.4 for pure DI water and net ion concentrations of ±0.7 mol L^{-1} for KCl under these applied voltages.

The local pH (or ion concentration) at the surface of an electrode can differ from that of the bulk solution by several orders of magnitude, affecting the energetics, reaction field strength, and kinetics of electrochemical reactions. Sensing the ion concentration at electrode surfaces is potentially important in controlling the selectivity of electrochemical and photoelectrochemical reactions, like CO_2 reduction, which normally compete with the hydrogen evolution reaction. There have been several previous attempts to quantify the local ion concentration at electrode surfaces. Using a rotating platinum disc electrode, Auinger *et al.* measured the near-surface ion distribution and buffer effects in electrochemical reactions including hydrogen oxidation (HOR) and hydrogen evolution reactions (HER).[1–3] While the ideal conditions utilized in this fundamental study cannot be directly applied to real scenarios, they do provide a basic understanding of the concept of surface pH for more complex heterogeneous reactions. Gupta *et al.* calculated the cathode surface concentrations in the electrochemical reduction of CO_2 in $KHCO_3$ solutions.[4] In this work, the authors predict a pH variation of 4.25 within 30 μm of the electrode surface. Deligianni *et al.* performed the first *in situ* measurement of surface pH during electrolysis using a rotating pH electrode.[5,6] Here, their spatial resolution was on the order of tens of microns. Using an optical approach, Leenheer and Atwater performed imaging of water-splitting electrocatalyst surfaces using pH-sensing confocal fluorescence microscopy.[7] Here, small concentrations of a pH indicator dye added to the aqueous electrolyte enabled ratiometric fluorescence sensing for quantitative pH detection over a relatively small pH range from 5.3 to 7.5, but with minimal perturbation to the local environment. While interesting, these previous attempts to establish the local pH near electrode surfaces have been inaccurate, invasive, and/or do not provide small enough spatial resolution to be considered "close" enough to the electrode to be relevant to the reaction of interest.

Our approach exploits the following unique properties of graphene: (1) single atomic layer thickness, (2) high Raman scattering cross-section, (3) small density of electronic states, and (4) large electron–phonon coupling strength, which make graphene's vibrational modes quite sensitive to charge density. All these combined properties provide an accurate measurement of the charge induced in the graphene electrode under electrochemical working conditions.

[a]Department of Chemistry, University of Southern California, Los Angeles, CA 90089, USA. E-mail: scronin@usc.edu
[b]Ming Hsieh Department of Electrical Engineering, University of Southern California, Los Angeles, CA 90089, USA
[c]Department of Materials Science, University of Southern California, Los Angeles, CA 90089, USA

†Electronic supplementary information (ESI) available. See DOI: 10.1039/c7nr08294k

Monolayer graphene is grown by chemical vapor deposition (CVD) on copper foil at 1000 °C in methane and H_2 gas at a reduced pressure of 1–1.5 Torr.[8] After growth, the copper foil is spin-coated with PMMA-A6 at 2000 rpm for 45 s and then baked at 150 °C for 5 minutes. The copper foil is then etched away in copper etchant, and the graphene with PMMA is "scooped" out and rinsed in 10% HCl and DI water. Next, the graphene monolayer is transferred to the target substrate with the same scooping method and baked at 120 °C for 5 minutes to improve adhesion. After this, the PMMA layer is removed with a 5-minute acetone dip.[9] Prior to transferring the graphene, two gold electrodes are deposited on a glass slide by electron-beam evaporation using a shadow mask. After transferring the graphene to these electrodes, copper wires are connected to the gold electrodes and epoxy is used to cover the surface of the gold electrode so that only the graphene electrode is in contact with the electrolytic solution. After the protection of the epoxy the active graphene area was about 1 cm^2. Raman spectra (532 nm excitation) of the graphene electrode under applied electrochemical potentials are taken in liquid solutions consisting of pure DI water and 1 M KCl using a water immersion lens, as illustrated in Fig. 1a. In order to protect the lens from the solution, a 13 μm thick Teflon sheet (American Durafilm Inc.) was used to cover the lens. Three terminal potentiostat (Gamry, Inc.), as illustrated in Fig. 1a, is used to add bias between our graphene working electrode and the reference electrode. A glassy carbon (SPI, Inc.) and a Ag/AgCl reference electrode were used as the counter electrode and reference electrode, respectively. Three-terminal potentiostat setup eliminates errors associated with voltage drops across the low conductivity DI water. Electrochemical impedance measurements were also carried out using the electrochemical impedance spectroscopy the three-terminal potentiostat (Gamry, Inc.).

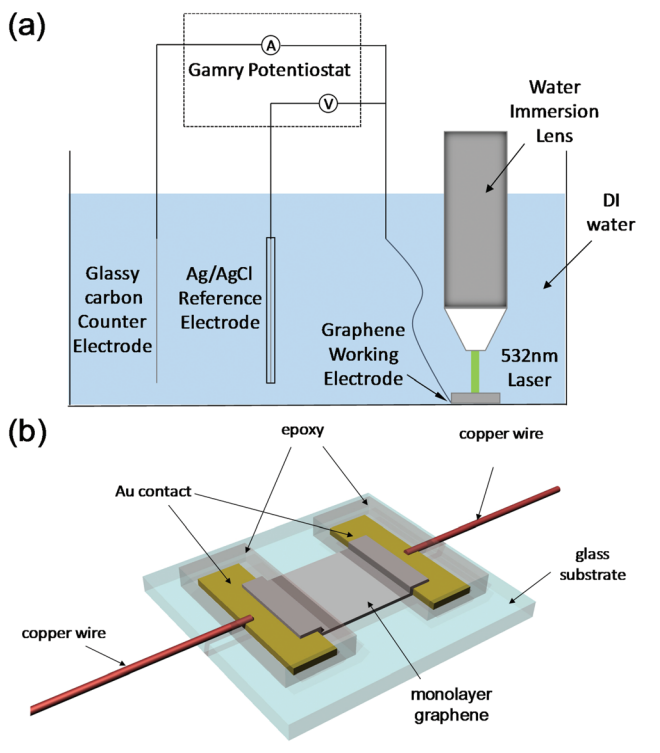

Fig. 1 (a) Schematic diagrams of the three-terminal photoelectrochemical cell using a water immersion lens and (b) monolayer graphene electrode.

Fig. 2 shows the G band Raman shift measured as a function of the applied voltage measured in a three-terminal electrochemical cell. Here, we observe substantial upshifts in the G band Raman frequency for both positive and negative applied potentials. Using the relation between Fermi energy (E_F) and doping concentration (n) obtained by Das Sarma *et al.*, $E_F = 11.65\sqrt{\tilde{n}}$ (meV, in which $\tilde{n} = n/10^{10}$ cm^{-2}),[10] and the linear relation between E_F and $\Delta\omega_G$ (with slightly different slopes observed for electron and hole doping),[11] we also plot the charge concentration in the graphene as a function of the applied voltage on the right axis of Fig. 2a.[12] Here, we see that the charge neutrality point occurs at 0.0 V *vs.* NHE. For voltages above this charge neutrality point, the ions in solution are OH^- ions, and for voltages below this, the ions are H_3O^+. At the charge neutrality point, we expect the ion concentration at the surface of the electrode to reach a minimum (*i.e.*, the point of minimum charge in solution). In this plot, we also indicate the Fermi energy of the graphene on the top horizontal axis, which spans a range from −430 meV to +390 meV. It should be noted that graphene, because of its linear dispersion relation and constant density of electronic states, provides a convenient system with linear relationships between the G band frequency, applied voltage, and Fermi energy, and a quadratic relationship between Fermi energy and doping concentration. Furthermore, because of graphene's small electron density of states, the Fermi energy of this material can be tuned over a large range of ±430 meV. Results of more than one samples shows the range of charge neutrality point is less than 0.1 V. See Fig. S1(b).† Fig. 2b shows the G band linewidth plotted as a function of applied voltage, which varies from 15.2 cm^{-1} at the charge neutrality point to 6.3 cm^{-1} for heavily doped graphene. These results are consistent with previous reports of Yan *et al.*[12,13] and arise from a Kohn anomaly,[14,15] which causes the G band to be broadened and downshift near the charge neutrality point of graphene.[16–20]

Fig. 3 shows the corresponding Raman data taken with the monolayer graphene electrode in a 1 M KCl solution. Again, we see substantial upshifts (up to 18 cm^{-1}) in the G band Raman frequency under both positive and negative applied potentials, as observed in the DI water solution (Fig. 2). However, here, the charge neutrality point occurs at +0.2 V *vs.* NHE, indicating doping of the graphene due to the ions in solution at zero applied potential. Here, the charge density on the graphene reaches $\pm 1.2 \times 10^{13}$ cm^{-2} under the applied potentials in this range. Again, we see a substantial drop in the G band linewidth from 15.2 cm^{-1} at the charge neutrality point to 6.3 cm^{-1} when heavily doped, corresponding to doping-induced suppression of the Kohn anomaly.

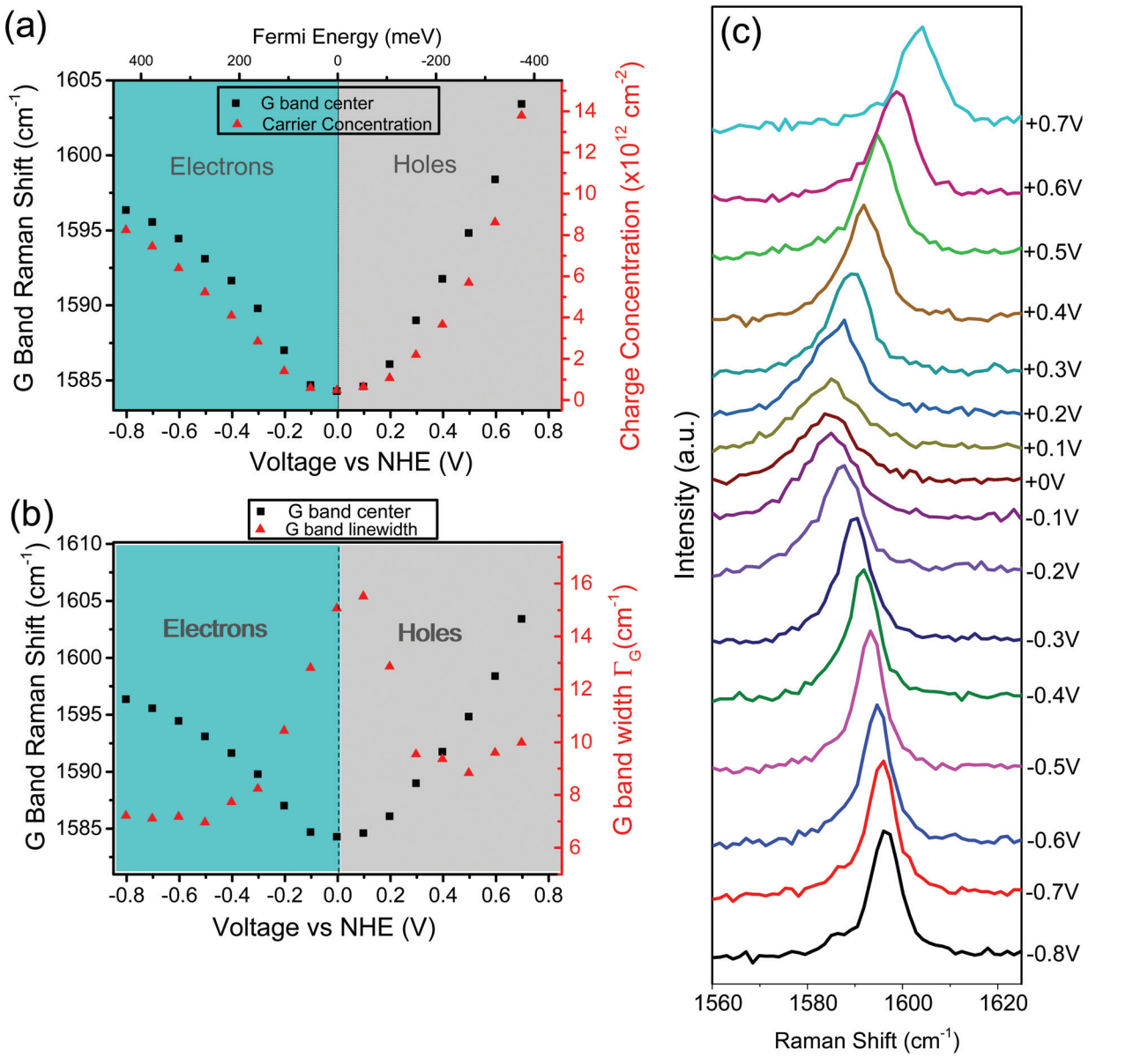

Fig. 2 (a) G-band Raman shift and corresponding charge concentration and (b) G band Raman linewidth plotted as a function of the applied voltage and Fermi energy measured in DI water. (b) Raw spectra showing the voltage-induced redshift of the G-band Raman mode.

We also quantified the graphene charge concentration (and hence ion concentration) using electrochemical impedance (EIS) measurements, which provide the capacitance–voltage relation at the electrode/electrolyte interface, as shown in Fig. 4a. The charge (and carrier density) can then be obtained from these capacitance–voltage characteristics (*i.e.* $Q = CV$). See Fig. S2 in the ESI† for further details. The Fig. 4a shows the capacitance–voltage plot of the graphene electrode measured in both DI water and 1 M KCl. Here, the capacitance–voltage profiles both exhibit a dip near the minimum charge point, as observed with Hg electrodes.[21–23] The charge density per unit area obtained from the product of the capacitance and voltage (*i.e.*, $Q = CV$) is plotted as a function of the applied potential for the DI water and 1 M KCl solutions in Fig. 4b and c, respectively. Here, the charge density is plotted together with the charge density obtained by Raman spectroscopy, and we observe excellent agreement between these two independent measurements of charge in this graphene electrode system. The agreement is particularly good near the charge neutrality point. However, discrepancies occur at relatively high potentials, likely due to non-linearities in the $\Delta n/\Delta\omega_G$ relation for heavily doped graphene. Here, the capacitance is roughly a factor of two larger in the KCl solution than in pure DI water, as expected due to the short ion distribution (*i.e.*, Debye length) in the ionic solution.

In order to estimate the local ion concentration at the electrode surface, we assume that the ions in solution follow an exponential distribution as a function of distance from the

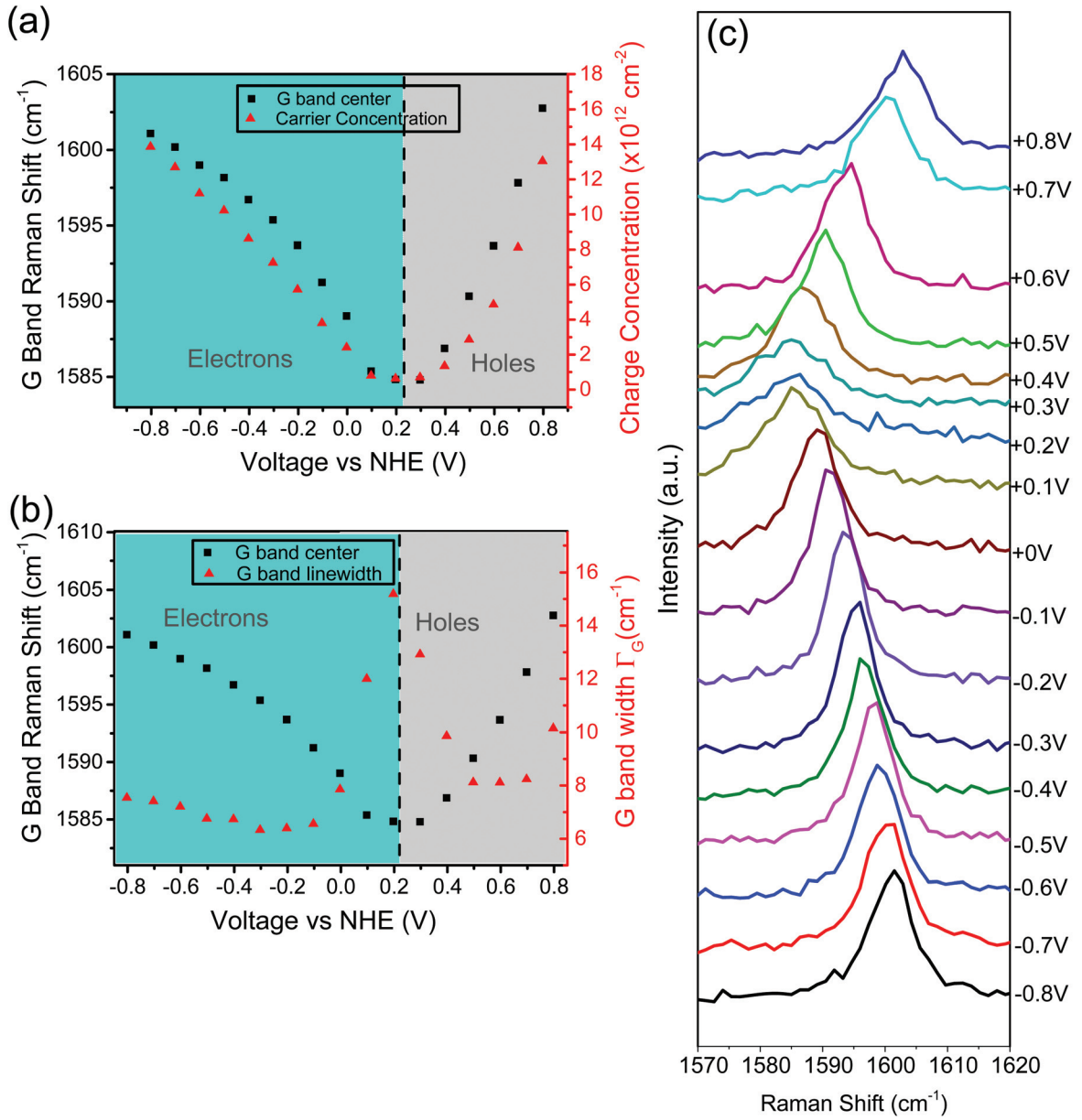

Fig. 3 (a) G band Raman shift and corresponding charge concentration and (b) G band Raman linewidth plotted as a function of the applied voltage and Fermi energy measured in 1 M KCl solution. (c) Raw Raman spectra showing the voltage-induced redshift of the G band Raman mode.

electrode surface with a decay constant given by the Debye length of the solution. For DI water, λ_D = 961 nm and for 1 M KCl, λ_D = 0.3 nm. From charge neutrality requirements, we set the ion concentration in solution per unit area equal (and opposite) to the charge density in the graphene electrode, *i.e.*, $n_G = \int_0^\infty A_0 \exp\left(-\frac{z}{\lambda_D}\right) dz = A_0\lambda_D$, where n_G is the charge density in the graphene electrode and A_0 is the charge density at the interface, which can be obtained by the ratio n_G/λ_D. Fig. 5 shows the local ion concentration plotted as a function of the applied potential for both pure DI water and 1 M KCl solution. From these ion distributions, we determine the local pH, which spans a range from 3.8 to 10.4 for pure, pH neutral water under these applied voltages as plotted in Fig. 5b. For the 1 M KCl solution, the net local ion concentration spans a range of ±0.78 mol L^{-1} under these applied voltages, as plotted in Fig. 5c. It is important to note that, in DI water, this approach provides a direct measure of the local pH. In electrolytic solutions (*e.g.*, KCl), however, the charge on the electrode (*i.e.* graphene) will be a sum of the ions in solution (*i.e.* H^+, $K^{+)}$. However, in 1 M KCl, the H^+ ion concentration is many (approximately seven) orders of magnitude smaller than K^+, and can be neglected. The same measurement was also carried out in 5 different solutions with pH values ranges from 0.58 to 12.70, as shown in Fig. S3a of ESI.† The comparison of the results of the local pH values calculated from the Raman

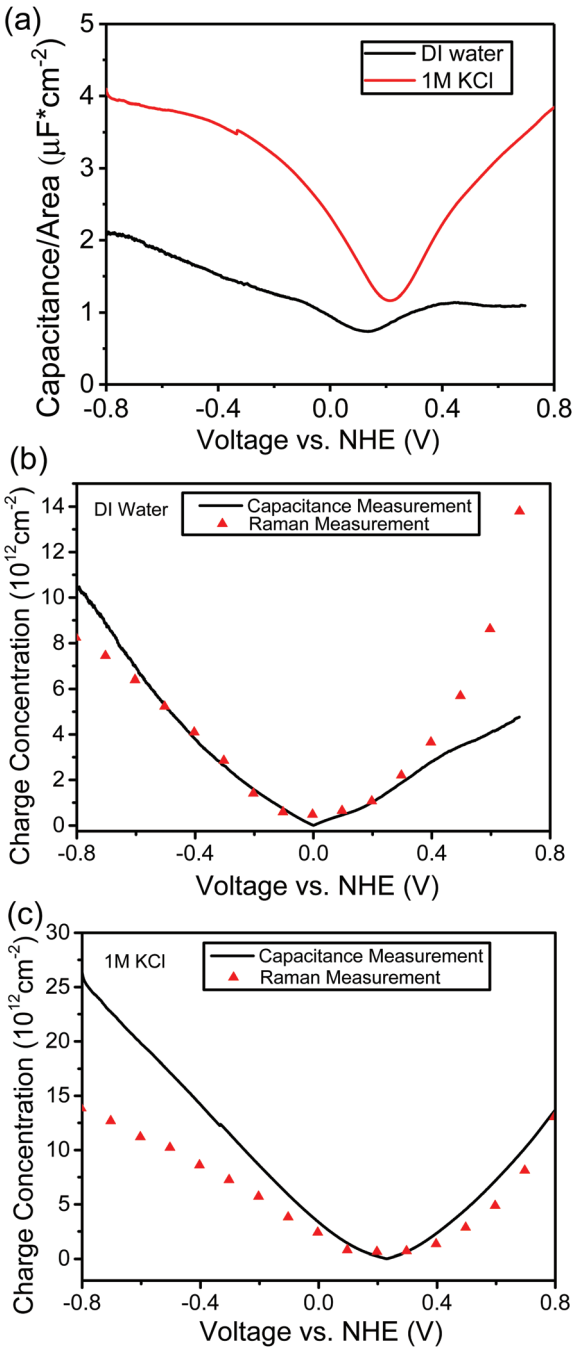

Fig. 4 (a) Capacitance–voltage plot of the graphene-based electrode measured in DI water and 1 M KCl. Charge densities obtained from the capacitance–voltage data (*i.e.*, $Q = CV$) and Raman spectroscopy in (b) DI water and (c) 1 M KCl.

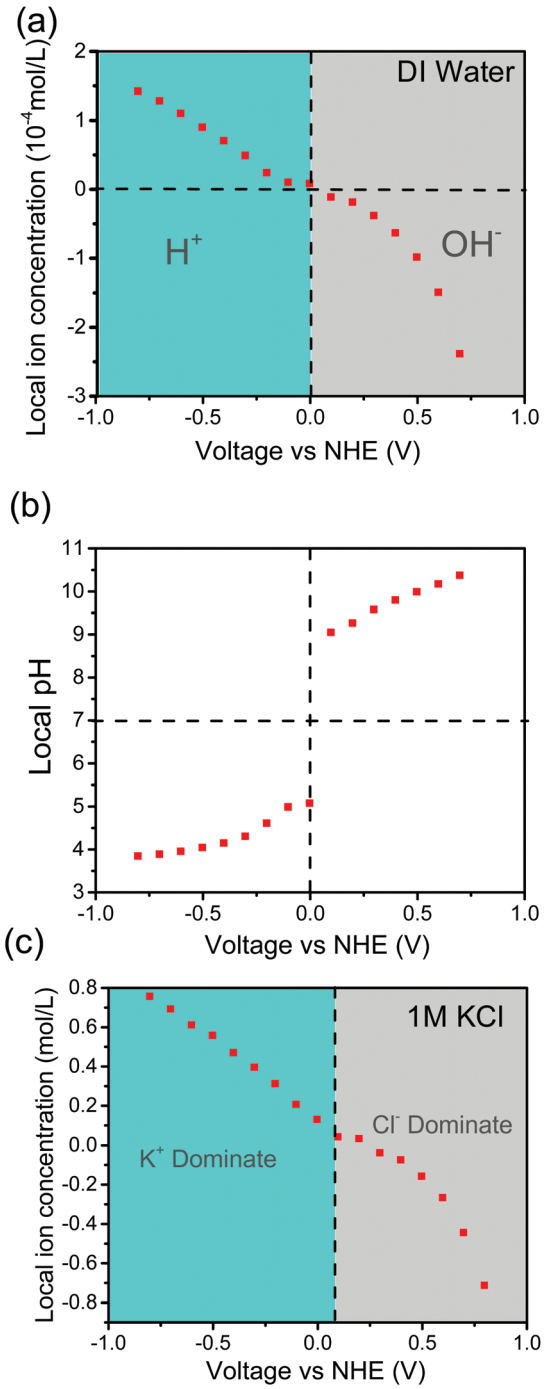

Fig. 5 Local ion concentration plotted as a function of voltage for (a) pure DI water and (c) 1 M KCl. (b) Local pH plotted as a function of voltage for pure DI water.

measurements with defined pH are shown in Fig. S3† as well. As we can see, the measured pH are very close to the defined pH values, which verifies the applicability of the proposed pH sensing method.

In summary, we have developed a technique for measuring the local ion concentration at graphene/water interfaces using Raman spectroscopy. Here, the charge density in the graphene sheet is determined from the upshifts in the G band Raman frequency. We observe upshifts as large as 19 cm^{-1} under applied potentials of ±0.8 V *vs.* NHE, which corresponds to charge densities of $\pm 1.4 \times 10^{13}$ cm^{-2} and Fermi energy shifts of ±430 meV. An independent measurement of the charge density in the graphene, based on the capacitance–voltage characteristics (*i.e.*, $Q = CV$) is found to be consistent with the Raman measurements, particularly near the charge neutrality point of graphene. The local ion concentration at the water/graphene

interface is estimated assuming the charge per unit area is equal and opposite to the charge density in the graphene electrode. The G band upshifts and, hence, ion concentrations are measured as a function of voltage in both pure DI water and 1 M KCl solutions. This type of local probing of ion concentration is potentially important in controlling the selectivity of electrochemical and photoelectrochemical reactions, like CO_2 reduction, which normally compete with the hydrogen evolution reaction.

Conflicts of interest

There are no conflicts to declare.

Acknowledgements

The authors would like to thank Drs. Joel Ager, Sri Narayan and Rehan Kapadia for valuable discussions. This research was supported by the Army Research Office ARO Award No. W911NF-14-1-0228 (H. S.), Air Force Office of Scientific Research Grant No. FA9550-15-1-0184 (B. H.), NSF Award No. CBET-1512505 (L. S.), and ACS-PRF grant #55993-ND5 (N. P.).

References

1 M. Auinger, I. Katsounaros, J. C. Meier, S. O. Klemm, P. U. Biedermann, A. A. Topalov, M. Rohwerder and K. J. J. Mayrhofer, *Phys. Chem. Chem. Phys.*, 2011, **13**, 16384.
2 I. Katsounaros, J. C. Meier, S. O. Klemm, A. A. Topalov, P. U. Biedermann, M. Auinger and K. J. J. Mayrhofer, *Electrochem. Commun.*, 2011, **13**, 634.
3 L. Rossrucker, A. Samaniego, J. P. Grote, A. M. Mingers, C. A. Laska, N. Birbilis, G. S. Frankel and K. J. J. Mayrhofer, *J. Electrochem. Soc.*, 2015, **162**, C333.
4 N. Gupta, M. Gattrell and B. MacDougall, *J. Appl. Electrochem.*, 2006, **36**, 161.
5 H. Deligianni and L. T. Romankiw, *IBM J. Res. Dev.*, 1993, **37**, 85.
6 L. T. Romankiw, *J. Electrochem. Soc.*, 1970, **117**, C118.
7 A. J. Leenheer and H. A. Atwater, *J. Electrochem. Soc.*, 2012, **159**, H752.
8 K. Soo Min, H. Allen, L. Yi-Hsien, D. Mildred, P. Tomás, K. Ki Kang and K. Jing, *Nanotechnology*, 2013, **24**, 365602.
9 C. C. Chen, C. C. Chang, Z. Li, A. F. J. Levi and S. B. Cronin, *Appl. Phys. Lett.*, 2012, **101**, 22.
10 S. Das Sarma, S. Adam, E. H. Hwang and E. Rossi, *Rev. Mod. Phys.*, 2011, **83**, 407.
11 G. Froehlicher and S. Berciaud, *Phys. Rev. B: Condensed Matter and Materials Physics*, 2015, **91**, 205413.
12 J. Yan, Y. Zhang, P. Kim and A. Pinczuk, *Phys. Rev. Lett.*, 2007, **98**, 166802.
13 M. Bruna, A. K. Ott, M. Ijas, D. Yoon, U. Sassi and A. C. Ferrari, *ACS Nano*, 2014, **8**, 7432.
14 S. Pisana, M. Lazzeri, C. Casiraghi, K. S. Novoselov, A. K. Geim, A. C. Ferrari and F. Mauri, *Nat. Mater.*, 2007, **6**, 198.
15 M. Lazzeri and F. Mauri, *Phys. Rev. Lett.*, 2006, **97**, 266407.
16 K. Sasaki, M. Yamamoto, S. Murakami, R. Saito, M. S. Dresselhaus, K. Takai, T. Mori, T. Enoki and K. Wakabayashi, *Phys. Rev. B: Condensed Matter and Materials Physics*, 2009, **80**, 155450.
17 K. Sasaki, H. Farhat, R. Saito and M. S. Dresselhaus, *Physica E*, 2010, **42**, 2005.
18 D. Yoon, D. Jeong, H. J. Lee, R. Saito, Y. W. Son, H. C. Lee and H. Cheong, *Carbon*, 2013, **61**, 373.
19 J. Binder, J. M. Urban, R. Stepniewski, W. Strupinski and A. Wysmolek, *Nanotechnology*, 2016, **27**, 045704.
20 A. Das, S. Pisana, B. Chakraborty, S. Piscanec, S. K. Saha, U. V. Waghmare, K. S. Novoselov, H. R. Krishnamurthy, A. K. Geim, A. C. Ferrari and A. K. Sood, *Nat. Nanotechnol.*, 2008, **3**, 210.
21 D. C. Grahame, *J. Am. Chem. Soc.*, 1954, **76**, 4819.
22 L. Balents and M. P. A. Fisher, *Phys. Rev. B: Condensed Matter and Materials Physics*, 1997, **55**, 11973.
23 N. Sato, *Electrochemistry at Metal and Semiconductor Electrodes*, Elsevier, 1998.

